Effect of Interfaces on the Alignment of a Discotic Liquid−Crystalline Phthalocyanine

ARTICLE *in* LANGMUIR · SEPTEMBER 2006

Impact Factor: 4.46 · DOI: 10.1021/la0605182 · Source: PubMed

Effect of Interfaces on the Alignment of a Discotic Liquid−Crystalline Phthalocyanine

Vinciane De Cupere,[†] Julien Tant,[†] Pascal Viville,[‡] Roberto Lazzaroni,[‡] Wojciech Osikowicz,[§] William R. Salaneck,[§] and Yves Henri Geerts*,[†]

Laboratory of Polymer Chemistry, CP 206/1, Université Libre de Bruxelles, Boulevard du Triomphe, 1050 Bruxelles, Belgium, Laboratory for Chemistry of Novel Materials, Université de Mons-Hainaut/ Materia Nova, Place du Parc, 20, B-7000 Mons, Belgium, and Department of Physics, IFM, Linköping University, S-58183 Linköping, Sweden

Received February 23, 2006

This paper deals with the influence of the nature and number of solid interfaces on the alignment of the columns in a semiconducting discotic liquid crystal. The solid substrates have been characterized in terms of their roughness and surface energy. The alignment of the discotic liquid crystal columns on these substrates has been determined by optical microscopy under crossed polarizers and by tapping-mode atomic force microscopy. The nature of the substrates has negligible influence on the alignment. The key parameter is the confinement imposed to the film. These surprising observations are explained by the antagonist alignment role of gas and solid interfaces.

1. Introduction

Discotic liquid crystals (DLCs) are currently viewed as a new generation of organic semiconductors with unique features that differentiate them from the more conventional conjugated polymers.[1] DLCs benefit from the easiness of solution processing with the advantage of having discrete molecular mass and defect-free chemical structure. Moreover, the strong interaction (due to the large contact area) between adjacent disks in columns results in bandwidths up to 1.1 eV,[2] high charge carrier mobility on the order of 0.1−1.0 $cm^2/V•s$,[3,4] and large exciton diffusion lengths exceeding 100 nm.[5] These performances exceed those of most conjugated polymers and qualify DLCs as functional materials for device applications in organic electronics. DLCs are quasi one-dimensional (1D) semiconductors, that is, charges and excitons travel much faster along columnar stacks than between columns.[6,7] This implies that the columnar stacks must be adequately aligned between electrodes. Planar or homogeneous alignment of columns, that is, parallel to the dielectric substrate, is needed in field-effect transistors,[8] whereas homeotropic alignment of columns, that is, perpendicular to electrodes, is required in photovoltaic cells[9] and light-emitting diodes.[10] Planar alignment has been achieved by drop-casting onto poly(tetrafluoroethylene)-rubbed surfaces,[11] by the zone casting technique,[12] and by vibrational excitation with pulsed infrared radiations on a film confined between two BaF_2 substrates.[13] Homeotropic alignment can be generated by thermal annealing, that is, upon slow cooling of the isotropic melt confined between two substrates.[14] Homeotropic alignment has been reported for some hexabenzocoronene (HBC),[15] phthalocyanine,[16,17] and triphenylene mesogens.[13,18−20] The latter almost systematically

* Corresponding author. E-mail: ygeerts@ulb.ac.be.
[†] Université Libre de Bruxelles.
[‡] Université de Mons-Hainaut/Materia Nova.
[§] Linköping University.

(1) (a) Simpson, C. D.; Wu, J.; Watson, M. D.; Müllen, K. *J. Mater. Chem.* **2004**, *14*, 494−504. (b) Eichhorn, H. *J. Porphyrins Phthalocyanines* **2000**, *4*, 88−102.

(2) Crispin, X.; Cornil, J.; Friedlein, R.; Lemaur, V.; Crispin A.; Kestemont, G.; Lehmann, M.; Fahlman, M.; Lazzaroni, R.; Geerts, Y.; Wendin, G.; Brédas, J.-L.; Salaneck, W. R. *J. Am. Chem. Soc.* **2004**, *126*, 11889−11899.

(3) (a) van de Craats, A. M.; Warman, J. M.; Müllen, K.; Geerts, Y.; Brand J. D. *Adv. Mater.* **1998**, *10*, 36−38. van de Craats, A. M.; Warman, J. M.; Fechtenkötter, A.; Brand, J. D.; Harbison, M. A.; Müllen K. *Adv. Mater.* **1999**, *11*, 1469−1472. Lehmann, M.; Kestemont, G.; Gómez Aspe, R.; Buess-Herman, C.; Koch, M. J. H.; Debije, M. G.; Piris, J.; de Haas, M. P.; Warman, J. M.; Watson, M. D.; Lemaur, V.; Cornil, J.; Geerts, Y. H.; Gearba, R.; Ivanov, D. A. *Chem.−Eur. J.* **2005**, *11*, 3349−3362. (b) An, Z.; Yu, J.; Jones, S. C.; Barlow, S.; Yoo, S.; Domercq, B.; Prins, P.; Siebbeles, L. D. A.; Kippelen, B.; Marder, S. R. *Adv. Mater.* **2005**, *17*, 2580−2583. Lino, H.; Takayashiki, Y.; Hanna, J. I.; Bushby, R. J. *Jpn. J. Appl. Phys.* **2005**, *44*, L1310−L1312.

(4) Lemaur, V.; da Silva Filho, D. A.; Coropceanu, V.; Lehmann, M.; Geerts, Y.; Piris, J.; Debije, M. G.; van de Craats, A. M.; Senthilkumar, K.; Siebbeles, L. D. A.; Warman, J. M.; Brédas, J. L.; Cornil, J. *J. Am. Chem. Soc.* **2004**, *126*, 3271−3279.

(5) Markovitsi, D.; Lécuyer, I. *J. Chem. Soc., Faraday Trans.* **1991**, *87*, 1785−1790. van Nostrum, C. F.; Bosman, A. W.; Gelinck, G. H.; Schouten, P. G.; Warman, J. M.; Kentgens, A. P. M.; Devillers, M. A. C.; Meijerink, A.; Picken, S. J.; Sohling, U.; Schouten, A. J.; Nolte, R. J. M. *Chem.−Eur. J.* **1995**, *3*, 171−182.

(6) Adam, D.; Schuhmacher, P.; Simmerer, J.; Häussling, L.; Siemensmeyer, K.; Etzbach, K. H.; Ringsdorf, H.; Haarer D. *Nature* **1994**, *371*, 141−3. van de Craats, A. M.; Warman, J. M.; de Haas, M. P.; Adam, D.; Simmerer, J.; Haarer, D.; Schuhmacher, P. *Adv. Mater.* **1996**, *8*, 823−826. Boden, N.; Bushby, R. J.; Clements, J.; Movaghar, B. *Phys. Rev. B* **1995**, *52*, 13724−13780. Piris, J.; Debije, M. G.; Stuzmann, N.; van de Craats, A. M.; Watson, M. D.; Müllen, K.; Warman, J. M. *Adv. Mater.* **2003**, *15*, 1736−1740.

(7) Markovitsi, D.; Lécuyer, I.; Simon, J. *J. Phys. Chem.* **1991**, *95*, 3620−3626. Hughes, R. E.; Hart, S. P.; Smith, D. A.; Movaghar, B.; Bushby, R. J.; Boden, N. *J. Phys. Chem. B* **2002**, *106*, 6638−6645.

(8) van de Craats, A. M.; Stutzmann, N.; Bunk, O.; Nielsen, M. M.; Watson, M. Müllen, K.; Chanzy, H. D.; Sirringhaus, H.; Friend, R. *Adv. Mater.* **2003**, *15*, 495−499.

(9) Schmidt-Mende, L.; Fechtenkötter, A.; Müllen, K.; Moons, E.; Friend, R. H.; MacKenzie, J. D. *Science* **2001**, *293*, 1119−1122.

(10) Lüssem, G.; Wendorff, J. H. *Polym. Adv. Technol.* **1998**, *9*, 443−460. Seguy, I.; Destruel, P.; Bock, H. *Synth. Met.* **2000**, *15*, 111−112.

(11) Bunk, O.; Nielsen, M. Sølling, T. I.; van de Craats, A. M.; Stutzmann, N. *J. Am. Chem. Soc.* **2003**, *125*, 2252−2258.

(12) Tracz, A.; Jeszka, K.; Watson, M. D.; Müllen, K.; Pakula, T. *J. Am. Chem. Soc.* **2003**, *126*, 1682−1683.

(13) Monobe, H.; Awazu, K.; Shimizu, Y. *Adv. Mater.* **2000**, *12*, 1495−1499.

(14) Fujikake, H.; Murashige, T.; Sugibayashi, M.; Ohta, K. *Appl. Phys. Lett.* **2004**, *85*, 3474−3476.

(15) (a) Pisula, W.; Tomovic, Z.; El Hamaoui, B.; Watson, M. D.; Pakula, T.; Müllen, K. *Chem. Mater.* **2005**, *17* (17), 4296−4303. (b) Pisula, W.; Tomovic, Z.; El Hamaoui, B.; Watson, M. D.; Pakula, T.; Müllen, K. *Adv. Funct. Mater.* **2005**, *15*, 893−904.

(16) Hatsusaka, K.; Otha, K.; Yamamoto, I.; Shirai, H. *J. Mater. Chem.* **2001**, *11*, 423−433. Hatsusaka, K.; Kimura, M.; Otha, K. *Bull. Chem. Soc. Jpn.* **2003**, *76*, 781−787.

(17) Lino, H.; Hanna, J. I.; Bushby, R. J.; Movaghar, B.; Whitaker, B. J.; Cook, M. *J. Appl. Phys. Lett.* **2005**, *87*, 132102-1−132102-3.

(18) Terasawa, N.; Monobe, H.; Kiyohara, K.; Shimizu, Y. *J. Chem. Soc., Chem. Commun.* **2003**, 1678−1679.

(19) Géminard, J. C.; Oswald, P. *J. Phys. II* **1994**, *4*, 959−974.

(20) Prasad, S. K.; Shankar Rao, D. S.; Chandrasekhar, S.; Kumar, S. *Mol. Cryst. Liq. Cryst.* **2003**, *396*, 121−139.

10.1021/la0605182 CCC: $33.50
Published on Web 05/23/2006

displays homeotropic alignment, both for films confined between two substrates[18,21] and for films deposited on one substrate.[22] Low isotropic melt viscosity associated with the presence of oxygen atoms in the flexible side chains have been postulated as key parameters for the homeotropic alignment of phthalocyanine mesogens.[16] Recently, the presence of a crown of perfluoroalkyl side chains in perfluoroheptyloxytriphenylene has been reported to induce homeotropic alignment on polyimide, indium tin oxide (ITO), and cetyltrimethylamonium bromide-coated glass surfaces. Surprisingly, the corresponding hydrocarbon homologue, that is, a heptyloxytriphenylene derivative, does not exhibit homeotropic alignment on the same series of substrates.[18] Another study has shown that several alkyloxytriphenylene derivatives, including the same heptyloxytriphenylene derivative, prefer homeotropic alignment between Si, CaF_2, ZnSe, and ZnS substrates. An anchoring transition has even been recorded as a function of thermal history.[21] Very recently, an alkylated hexa-peri-HBC mesogen containing no heteroatoms has also been found to homeotropically align.[15] From these scattered results, no obvious correlation seems to exist between the molecular structure and the occurrence of homeotropic alignment. We note, however, that the clearing temperature of those compounds, and hence the annealing conditions, vary considerably. In the particular case of DLCs, little attention has been paid to the surface energy and surface morphology of the substrates, although these parameters are known to govern the homeotropic alignment of calamitic liquid crystals.[23−25]

To contribute to the elucidation of the alignment mechanism and with the ultimate goal of fabricating solar cells with functional DLCs, we have undertaken a study of the alignment of phthalocyanine mesogens.[26] In this paper, we report on the orientation of phthalocyanine columns in thick (a few micrometers) or thin films (a few tens of nanometers) and on the influence of confinement on the occurrence of homeotropic alignment. Thin films are obtained by spin-coating solutions of a phthalocyanine derivative on one substrate while thicker deposits are prepared by melting the same phthalocyanine derivative between two identical substrates. The orientation of the columns in those films is characterized by polarized optical microscopy (POM) and by tapping-mode atomic force microscopy (TMAFM) as a function of the preparation method, the polarity and roughness of the substrates, and the number of DLC−solid interfaces (one or two).

2. Experimental Section

2.1. Materials. *2.1.1. Substrates.* Different types of substrates have been tested in this work. Their references or preparation methods are given hereafter. The glass plates used (76 × 26 mm) are a Marienfeld product distributed by VWR International (Haasrode, Belgium), ref: mari10000000. They were cut into 26 × 26 mm^2 pieces and immersed in a piranha mixture (1 H_2O_2 30% in water; 9 H_2SO_4) for 30 min, rinsed thoroughly with distilled water, and dried by spinning at 4000 rpm on the spin-coater for a few seconds.

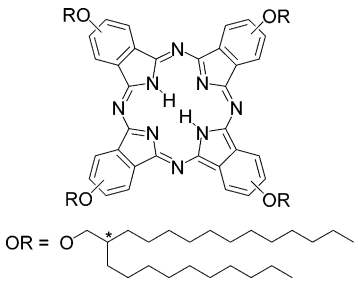

Figure 1. Chemical structure of mesogenic 4-fold substituted phthalocyanine (**Pc**), which exists as a mixture of four isomers: $D_{2h}/C_s/C_{2v}/C_{4h}$ with a statistical distribution 12.5:50:25:12.5. Alkoxy side chains were used as racemates.

The ITO plates used are a Merck product (Merck KGaA Germany; product number: 255 639x0; 14 × 14 in.; 100 nm ITO; 20 ohm/cm^2).

The gold substrates were prepared by depositing a thin gold layer (∼10 nm) on a 16 cm^2 glass substrate by direct current (dc) magnetron sputtering. The glass substrate was cleaned with RBS 25 prior to deposition. A gold disk (99.9% purity) 1.3 in. in diameter was used as the target, and the target−substrate distance was 15 cm. The base pressure in the deposition chamber was about 10^{-6} Torr. The sputtering gas was an argon/oxygen mixture, and the pressure was regulated with a throttle valve at 0.67 Pa. Two gas flow controllers maintained the Ar and O_2 flows in the chamber. An MDX 500 continuously variable power supply was used as the power source. The target current was set at 50 mA.

[6,6]-Phenyl-C_{61}-butyric acid methyl ester (PCBM; Nano-C, Westwood, MA; ref. PCBM-01, batch B-12−31−04), poly(4-styrenesulfonate)-doped poly(3,4-ethylenedioxythiophene) (PEDOT:PSS; Agfa Gevaert, Belgium), poly(isobutylene) (IR; Acros product, Geel, Belgium; ref 356060500, batch A0206854001; $M_w = 170\,000$), and fluorinated rubber (FKM; gift from Montefluos; $[(CH_2-CF_2)_{0.6}-(CF_2-CF(CF_3))_{0.4}]_n$; $M_w = 70\,000$) substrates were obtained by spin-coating on cleaned glass plates. The preparation conditions were as follows: PCBM was dissolved in toluene at a concentration of 4 mg/mL and spin-coated at 1500 rpm; PEDOT:PSS was provided as a colloidal solution in water and was spin-coated as such, at 1500 rpm; IR was dissolved in toluene at a concentration of 5 wt % and spin-coated at 6000 rpm; FKM was dissolved in acetone at a concentration of 10 wt % and spin-coated at 6000 rpm.

2.1.2. Discotic Liquid Crystal. The synthesis of 2(3),9(10),16(17),23(24)-tetra(2-decyltetradecyloxy)-phthalocyanine, abbreviated **Pc** (Figure 1), has been described elsewhere.[26a,b] The obtained product is a green pasty material with a columnar rectangular (Col_r) phase up to 60 °C (lattice parameters: $a = 52.1$ Å, $b = 32.5$ Å, measured at 27 °C), a columnar hexagonal (Col_h) phase up to 180 °C (lattice parameters: $a = 32.2$ Å, measured at 110 °C), where the isotropic phase is reached.[26a−c]

^{1}H NMR analysis showed no traces of organic contaminants. Thin-layer chromatography confirmed the absence of starting reagents or side products from the synthesis. The presence of nonorganic contaminants was checked by inductively coupled plasma (ICP) analysis. The concentration of all elements (see Supporting Information) was below the detection limit. The analysis was repeated three times on the same sample, and the results were averaged over three measurements. One noticeable exception was for Silicon (Si), which showed an average concentration of 80 mg/kg, which corresponds to one silicon atom per 12 000 discotic molecules.

Two potential main sources of Si contamination were envisaged: colloidal inorganic silicon particles eluted from the silica gel of chromatography columns or silicone grease. To discriminate between the two possible Si contamination sources, a **Pc** thin film was heated for 1 h between 100 and 130 °C, with the goal of favoring the migration of silicon grease, if present, to the surface of the film. The sample was then analyzed with a surface-sensitive technique: X-ray photoelectron spectroscopy (XPS). No trace of Si was detected. Moreover, the atomic ratios between carbon, oxygen, and nitrogen

(21) Vij, J. K.; Kocot, A.; Perova, T. S. *Mol. Cryst. Liq. Cryst.* **2003**, *397*, 531−544.
(22) Sergan, T.; Sonpatki, M.; Kelly, J.; Chien, L. C. *Mol. Cryst. Liq. Cryst.* **2001**, *359*, 245−257.
(23) Noble, A. R.; Kwon, H. J.; Nuzzo, R. G. *J. Am. Chem. Soc.* **2002**, *124*, 15020−15029.
(24) Smela, E.; Martínez-Miranda, L. J. *J. Appl. Phys.* **1995**, *77*, 1930−1933.
(25) Yu, T.; Peng, Z.; Ruan, S.; Xuan, L. *Thin Solid Films* **2004**, *466*, 326−330.
(26) (a) Tant, J. Ph.D. Thesis, University of Brussels, September, 2003. (b) Tant, J, Geerts; Y. H., Lehmann, M.; De Cupere, V. M.; Zucchi, G.; Laursen, B. W.; Bjørnholm, T.; Lemaur, V.; Marcq, V.; Burquel, A., Hennebicq, E.; Gardebien, F.; Viville, P.; Beljonne, D.; Lazzaroni R.; Cornil, J. *J. Phys. Chem. B* **2005**, *109*, 20315−20323 (See also correction: *J. Phys. Chem. B* **2006**, *110*, 39−3449). (c) Gearba et al. have reported, independently of us, slightly different lattice parameters and transition temperatures (see ref 41).

were very close to the expected ones (see Supporting Information). This indicates that the Si most probably originates from a few residual silica particles that are not surface active.

2.2. Preparation of the Films. *2.2.1. Thick Films.* Thick films were prepared by depositing a few milligrams of **Pc** on a substrate, heating on a hot stage to a temperature 20 °C above the isotropic transition temperature (200 °C), depositing a second plate on the molten liquid crystal, applying a slight pressure to spread the fluid film on the largest possible area, and cooling the obtained sandwiched film at a rate of 10 °C/min. The obtained films had a thickness ranging from 5 to 20 μm.

2.2.2. Thin Films. Thin **Pc** films were prepared by spin-coating from solutions prepared in toluene at concentrations varying from 5 to 30 mg/mL (for spin-coating on glass plates) or in heptane at a concentration of 30 mg/mL (for spin-coating on ITO, gold, PEDOT:PSS, and PCBM substrates). Spin-coating on IR proved to be impossible since the solvents of **Pc** are also efficient to dissolve IR. The samples were spun for 60 s at 1500 rpm with an acceleration of 0−1500 rpm in 10 s. The obtained films had a thickness ranging from 40 to 300 nm, as determined with AFM from the profile of a step between the clean substrate and the film.[26] The films were annealed by heating to 183 °C (in the isotropic phase) and cooling to ambient temperature at a controlled rate: 0.1, 1, 10, or 20 °C/min.

2.3. Characterization Techniques. *2.3.1. Optical Microscopy (OM).* The liquid crystal samples were studied with a Nikon Eclipse 80i microscope equipped with polarizing filters and a digital Nikon DS-5M camera. The images were treated with the Eclipse Net software (version 1.20.0 build 61). Heating of the samples was performed with a Mettler FP82 hot stage equipped with an FP80 controller.

2.3.2. Contact Angle Measurements. Contact angle measurements were performed on a home-built apparatus consisting of a sample holder placed horizontally in the center of the field of a digital camera and a syringe mounted with a thin needle, which is used to deposit drops of liquid on the sample. Images of each drop were recorded, and the contact angles were estimated by measuring the angle between the solid−liquid interface and the tangent to the liquid−air interface at the location where the three phases (solid, liquid, and air) meet.

2.3.3. Atomic Force Microscopy (AFM). The AFM microscope was operated in tapping mode to minimize the sample damage due to mechanical interactions between the AFM tip and the surface of the organic film. To further optimize the imaging of the DLCs, the ratio between the set point amplitude and the amplitude of the free-oscillating cantilever (A_{sp}/A_0) was adjusted to 0.9 to avoid an excessive loading force applied to the sample and possible squeezing of the material between the tip and the substrate. In these conditions, TMAFM can provide three-dimensional imaging of the surface morphology with very accurate lateral and vertical resolution without damaging the surface. All TMAFM images were recorded in ambient atmosphere at room temperature with a Nanoscope IIIa (Veeco, Santa Barbara, CA) microscope. The probes were commercially available silicon tips with a spring constant of 24−52 N/m, a resonance frequency lying in the 264−339 kHz range, and a typical radius of curvature in the 10−15 nm range. The images were recorded with the highest available sampling resolution, that is, 512 × 512 data points.

3. Results and Discussion

3.1. Characterization of Substrate Surfaces. Seven substrates that significantly differ in terms of their surface energy and roughness were used in this study. Their water (Θ_w) and hexadecane (Θ_h) contact angles as well as their root-mean-square (RMS) roughness, as determined by TMAFM, are collected in Table 1. Water was chosen because it is the usual liquid for contact angle measurements, whereas hexadecane was selected because of its similarity with the alkyl side chains of **Pc**. Films of **Pc** display $\Theta_w = 94 \pm 4°$, typical of a hydrophobic surface. This indicates that the alkyl chains, which constitute a large part of the molecule, govern the interface properties of the material. Indeed, this value for Θ_w is identical to that of polyethylene.[27]

Table 1. Summary of the Physical Properties of the Substrates Used in This Study

substrate	contact angle of water[a]	contact angle of hexadecane[a]	surface roughness (RMS)[b]
glass	15 ± 1°	7 ± 2	3.2 ± 0.3 nm
IR	87 ± 1°	n.d.	0.6 ± 0.2 nm
ITO	66 ± 6°	6 ± 2	3.5 ± 0.5 nm
FKM	81 ± 4°	31 ± 3	0.5 ± 0.4 nm
PCBM	78 ± 6°	5 ± 1	1.0 ± 0.3 nm
PEDOT:PSS	19 ± 4°	12 ± 2	1.8 ± 0.3 nm
gold	54 ± 4°	9 ± 3	3.6 ± 0.3 nm

[a] Mean values and standard deviations of five measurements on the same sample. [b] RMS roughness measured in TMAFM for 5 × 5 μm^2 areas.

As expected, surfaces able to form hydrogen bonds (e.g., glass and PEDOT:PSS) display the lowest Θ_w values: 15° and 19°, respectively. The measured contact angle of water on ITO is, however, much higher (Θ_w = 66°), which is in very good agreement with the value of 60° measured by Kim et al.[28] The surface chemical composition of pristine ITO was described by Armstrong et al[29] and consists mainly of In_2O_3.

Gold surfaces display a water contact angle of 54°. This value is in good agreement with the study of Bartell and Smith,[30] who demonstrated that gold surfaces exposed to ambient atmosphere become rather rapidly contaminated by adsorbed organic molecules present in the atmosphere, with the consequence that the initial value of Θ_w in the absence of air, that is, 7°, raises rapidly to values around 65°. IR and PCBM display the highest water contact angles, Θ_w = 87° and 78°, respectively, as expected for materials containing mainly carbon and hydrogen atoms. FKM is a fluorinated material, is also hydrophobic, and exhibits a value of Θ_w = 81°.

Globally, the contact angles of hexadecane are lower than those of water. This is related to the intrinsic lower surface tension of this liquid (29.5 mN/m,[31] compared to 72 mN/m for water). The values range in a very small interval (from 5° for PCBM to 12° for PEDOT:PSS), except for FKM substrates for which a value of Θ_h = 31° is observed. This indicates that alkyl chains are rather insensitive to the chemical structure of the substrate they interact with, except for the introduction of fluorinated moieties. In this case, the solid−liquid interface tension increases due to the poor affinity between hydrocarbons and fluorocarbons.

The RMS roughness is defined as the standard deviation of the surface topography with respect to the mean height. It is calculated from the height of all the data points contained in the AFM image. The roughness values of the different substrates are collected in Table 1. These values are small (below 4 nm for 5 × 5 μm^2 images). For PCBM, IR, and FKM, the roughness is below 1 nm, as often found for organic layers obtained by spin-coating. Higher values are measured for glass (3.2 nm), ITO (3.5 nm), and gold (3.6 nm). These data are in good agreement with those reported in the literature: Armstrong et al[29] and Kim et al[28] measured roughness ranging between 0.5 and 3 nm for as-received ITO. Hammiche and Webb measured vertical variations

(27) Wu, S. *Polymer Interface and Adhesion*; Dekker: New York, 1982.
(28) Kim, J. S.; Friend, R. H.; Cacialli, F. *J. Appl. Phys.* **1999**, *86* (5), 2774−2278.
(29) Armstrong, N. R.; Carter, C.; Donley, C.; Simmonds, A.; Lee, P.; Brumbach, M.; Kippelen, B.; Domercq, B.; Yoo, S.; *Thin Solid Films* **2003**, *445*, 342−352.
(30) Bartell, F. E.; Smith, J. T. *J. Phys. Chem.* **1953**, *57*, 165−172.
(31) Nicolas, J. P.; Smit, B. *Mol. Phys.* **2002**, *100* (15), 2471−2475.

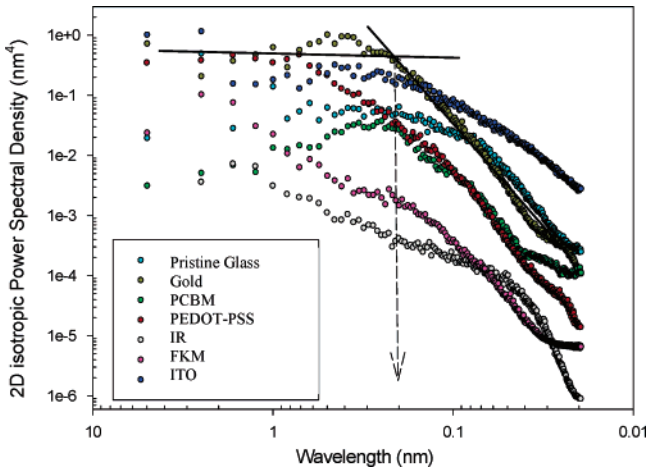

Figure 2. Averaged 2D isotropic PSD analysis of (5×5 μm^2) TMAFM images of the different substrates deposited on glass.

of the profile of gold films between 2 and 8 nm.[32] Those larger roughness values are related to the microcrystalline nature of ITO and gold. PEDOT:PSS deposits are also somewhat rough (1.8 nm here; 3 nm in ref 33), probably because of the colloidal nature of the PEDOT:PSS solutions. It has to be noted that the topographic profile of the substrates used in this study is not structured, that is, no groove or other specific pattern is present.

The scaling behavior of the surface roughness of the different substrates (the evolution of their surface roughness as a function of the lengthscale of observation) was also addressed via the analysis of the power spectral density (PSD) of the AFM images. PSD analysis allows one to determine the contribution to the surface topography from different spatial frequencies. From the Wiener−Kinchine theorem (eq 1), the integrated PSD yields the surface RMS roughness versus lengthscale r:

$$\sigma(r) = [\int_{1/r}^{f_{max}} PSD(f) f df]^{1/2} \quad (1)$$

where the high-frequency limit $f_{max} = N/2L$ (the Nyquist frequency), with N being the number of pixels per scan line and L being the image size.

The PSD analysis of the AFM images was carried out here to compare the scaling behavior of the surface roughness for the different substrates and to determine their typical surface correlation length, which can be related to the average size of the surface features.

From the average PSD spectra shown in Figure 2, one can first observe that the PSD maximum intensity varies over 3 orders of magnitude between the curve for IR and that for gold. This reflects the fact that IR shows the flattest surface and gold shows the roughest one, confirming the RMS values reported in Table 1.

The scaling behavior of the surface roughness is also very different depending on the nature of the substrate. A typical PSD spectrum classically exhibits a power-law dependence over a finite frequency range, corresponding to the linear correlated part of the spectrum. For instance, in the case of gold, this corresponds to the black straight line on the right part of the curve. Beyond this correlated part, surfaces that are made of well-defined features (for instance, grains with rather homogeneous size in the case of gold) exhibit a low-frequency plateau (horizontal line on Figure 2) representing the breakdown of the correlation. The onset of this plateau (marked by the dashed arrow) corresponds to the typical correlation length ξ of the objects observed on the surface (here, the size of typical morphological features of the gold surface). In contrast, surfaces that are featureless do not exhibit such a clear breakdown of the correlation; the PSD curve then appears to be smoother over a longer range of frequencies (for instance, FKM). The determination of a correlation length becomes irrelevant in such a case.

The PSD curves shown in Figure 2 thus not only confirm that the average surface roughness is different for the studied substrates, but also demonstrate that this roughness scales differently as a function of the lengthscale. The influence of the surface roughness and the correlation length on the alignment of phthalocyanine molecules is discussed in the following sections.

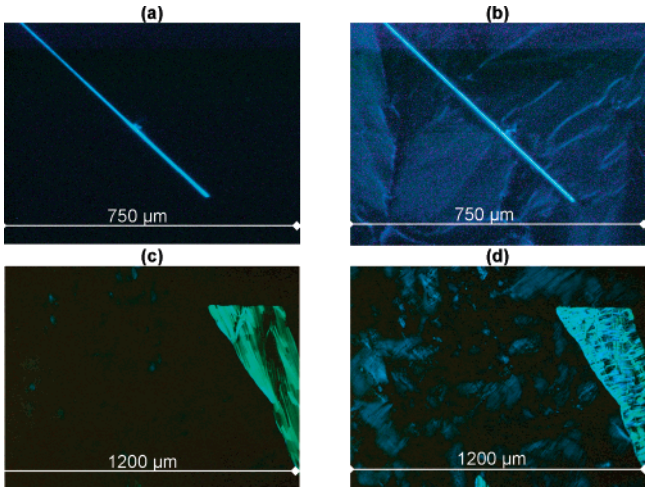

Figure 3. OM images under crossed polarizers obtained after annealing a **Pc** film between two glass plates (a,b) or between two FKM plates (c,d): (a,c) columnar hexagonal phase at 160°C; (b,d) rectangular phase at 40°C.

3.2. Films Formed between Two Plates. OM images recorded between crossed polarizers for **Pc** films formed between two glass plates with a cooling rate of 10°/min (thickness ranging from 5 to 20 μm) are presented in Figure 3. In the Col_h phase at 160 °C (Figure 3a), the film appears totally dark with some bright straight lines, independent of the rotational position of the sample between the polarizer and the analyzer. This absence of texture is commonly associated with the homeotropic alignment. Indeed, the Col_h phase possesses only one optical axis, which is parallel to the column axis. If the columns are perpendicular to the substrate, the incident light is parallel to the optical axis, and the material displays only one index of refraction. As a consequence, the polarized light travelling through the sample does not rotate and is totally stopped by the analyzer.[34] Bright straight lines, which are common defects of homeotropic alignment, are disclinations from which the new mesogenic phase starts to grow.[35] In the Col_r phase at 40 °C (Figure 3b), the film becomes dark blue. The bright straight lines are preserved, but some slight defects appear in the dark blue regions. The homogeneous dark blue color indicates that the orientation of the columns perpendicular to the substrates, which is observed in the Col_h phase, is globally preserved in the Col_r phase. The occurrence of small additional defects can be explained by the biaxiality of the Col_r phase, which induces the appearance of a

(32) Hammiche, A.; Webb, R. P. *Vacuum* **1994**, *45* (5), 569−573.
(33) Snaith, H. J.; Kenrick, H.; Chiesa, M.; Friend, R. H. *Polymer* **2005**, *46*, 2573−2578.
(34) Dierking, I. *Texture of Liquid Crystal*; Wiley-VCH: Weinheim, Germany, 2003.
(35) Pieranski, P.; Oswald, P. *Les Cristaux Liquides: Concepts et Propriétés Physiques Illustrés par des Expériences*, tome 2; G & B Science Publishers: Paris, France, 2002.

weak birefringence. For the sake of clarity, this peculiar alignment will be called "pseudohomeotropic" hereafter.

Similar optical observations have been made on ITO, PEDOT:PSS, PCBM, Au, and IR substrates, indicating that the alignment is also homeotropic. In contrast, on FKM, we did not observe complete homeotropic alignment. In this case, the phthalocyanine film (Figure 3c,d) also appears dark at 160 °C but, at some places, highly birefringent domains are observed. When cooling the film to 40 °C, slight defects develop in the dark part of the image, and the birefringent texture evolves, confirming the transition from Col_h to Col_r. From such observations, it can be deduced that the FKM does not induce a specific alignment; that is, while a major part of the film is constituted by columns perpendicular to the substrate, there are also large domains where it is not the case.

When paralleled to the data reported above for the native substrates (Table 1 and Figure 2), these optical observations indicate that the nature of the substrate does not have any influence on the development of homeotropic alignment. Surprisingly, homeotropic alignment is observed in every case, that is, for substrates that present very different surface roughness and surface correlation lengths as well as different surface energies.

The influence of the substrate roughness on the alignment of discotic molecules has hardly been studied in the literature. Van de Craats et al[8] and Zimmermann et al[36] demonstrated that the use of rubbed poly(tetrafluoroethylene) (PTFE) induces homogeneous alignment of HBC. They attributed such alignment to epitaxy rather than to a controlled roughness effect. No other surface-induced homeotropic organization has been described up to now for discotic molecules. For rodlike molecules, a large number of studies are available; they show that the substrate roughness plays an important role on the orientation of the molecules. Periodic topographic profiles with sinusoidal variations characterized by a 7.5−15 nm amplitude were demonstrated to vertically orient calamitic mesogens in the nematic and the smectic phases, while surfaces with random roughness of the same amplitude were inefficient to induce orientation.[37] Grooves with a depth of 1.5 μm and a period of 9−24 μm were shown to orient calamitic molecules parallel to the walls of the gratings.[38] Those examples suggest that anisotropic, oriented roughness is much more efficient in organizing liquid crystal molecules.

In our study, all the surfaces present an isotropic, nonperiodic roughness profile, and the average correlation length always largely exceeds the diameter of the phthalocyanine disk, meaning that all surfaces appear completely flat at the lengthscale of the molecules. This is probably the reason homeotropic alignment is always observed: this type of surface profile is expected to allow the formation of micrometer-long, perpendicular columns since the phthalocyanine disks can easily deposit flat on the surface and stack vertically from there over considerable lengthscales.

The lack of correlation between the molecular structure of DLCs and the occurrence of homeotropic alignment has been pointed out in the Introduction. This can be extended here to the chemical structure of the substrates sandwiching thick films of **Pc**. With the noticeable exception of FKM, which hardly differentiates homeotropic and planar alignment, all substrates induce homeotropic alignment regardless of their surface energy. It is therefore proposed that the sum of London dispersion forces

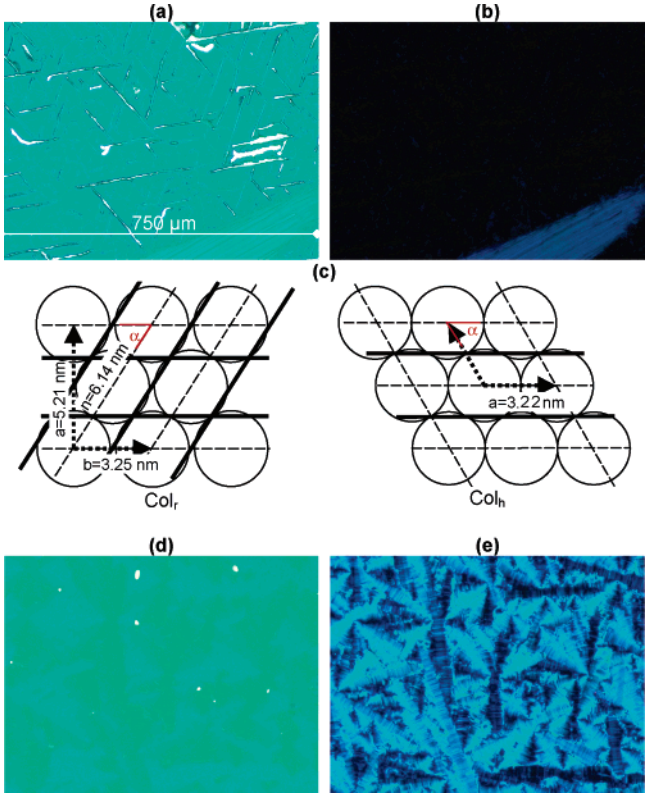

Figure 4. OM images of a **Pc** film confined between two glass plates after the separation of the two substrates at room temperature: A single plate observed with (a) normal light and (b) under crossed polarizers. (c) rectangular and hexagonal lattices, with the atom planes represented by the dotted lines, the fracture planes represented by the bold continuous lines, and the angle between the fracture planes labeled α. A single plate after annealing (heating to 200 °C and cooling at 10 °C/min) observed with (d) normal light and (e) under crossed polarizers.

between the molecules and the substrate, which are present with all substrates, overwhelms dipolar and multipolar interactions, which are present only with the polar substrates, and drives the alignment.[39] Therefore, the more or less polar character of the surface has no influence. It is worth noting that homeotropic alignment is also observed between two glass slides for a 3:1 blend of **Pc** with a lath-like, electron-accepting perylenetetracarboxydiimide derivative forming columnar mesophases.[40] This observation corroborates the view that homeotropic alignment is not governed by dipolar and multipolar interactions, at least for large discotic structures with hundreds of atoms in alkyl side chains.

3.3. Films Obtained after the Separation of the Two Plates. As described in the previous section, the presence of two confining plates drives the film of **Pc** into a homeotropic columnar arrangement. When those two plates are separated at room temperature, most of the material remains on one plate, creating a continuous layer with a few holes (Figure 4a,b) and a thickness similar to that of the original film. The sample appears totally dark under crossed polarizers (Figure 4b), indicating that homeotropic alignment has been preserved despite the stress applied during the separation of the plates. The deposit shows a pattern made of straight lines intersecting with angles of about 60 or 120°, which can be attributed to fractures occurring into

(36) Zimmermann, S.; Wendorff, J. H.; Weder, C. *Chem. Mater.* **2002**, *14*, 2218−2223.
(37) Nesrullajev, A.; Tepe, M.; Kazanci, N. *J. Appl. Phys.* **2002**, *35*, 2994−3001.
(38) Smela, E.; Martinez-Miranda, L. J. *J. Appl. Phys.* **1993**, *73* (7), 3299−3304.
(39) Arikainen, E. O.; Boden, N.; Bushby, R. J.; Lozmann, O. R.; Vinter, J. G.; Wood, A. *Angew. Chem., Int. Ed.* **2000**, *39* (13), 2333−2336.
(40) Zucchi, G.; Donnio, B.; Geerts, Y. H. *Chem. Mater.* **2005**, *17* (17), 4273−4277.

the film during the separation of the two substrates. Fractures occur preferentially along the directions of the cleavage planes of the material, which is in the rectangular phase at room temperature. The rectangular phase of **Pc** is expected to show fracture angles of 58 and 122°, as calculated from the lattice parameters (Figure 4c). This confirms that, even in the rectangular phase, the columns are perpendicular to the substrates.

When annealing (heating to 200 °C and cooling at 10 °C/min) is applied to the **Pc** films after separation of the glass plates, a new highly birefringent texture forms (Figure 4d,e), which is characteristic of a planar alignment. This observation strongly contrasts with the fact that annealing of the film sandwiched between two plates (i.e., before separation) leads to homeotropic alignment. Under the same annealing conditions, the occurrence of homeotropic alignment is thus related to the presence of the upper substrate, which induces a confinement of the liquid crystal film. This requirement of an upper substrate for obtaining homeotropic alignment has also been observed by Pisula et al[15a] for some all-hydrocarbon HBC derivatives. The same group also reported what appears to be an exception: a structurally comparable HBC derivative, except for the presence of one ether link per lateral alkyl chain, homeotropically aligns in thin films with one air interface.[15b] Such alignment could only be obtained for one specific mesogen and for an appropriately small film thickness. However, no value of thickness was given.

The influence of the number and nature of substrates on the organization of phthalocyanine molecules was further investigated by means of TMAFM. The characterization of the films molten between two substrates was made possible by separating the two glass plates. Figure 5a shows the typical morphology of the film directly after the substrate separation. On the micrometer scale, the surface of the film also locally exhibits straight lines intersecting with angles of about 60 or 120°, as pointed by the white arrows in Figure 5a. At higher resolution, the surface of the film is totally featureless and no signature of a planar columnar arrangement (i.e., columns lying flat on the surface) has been found on this system (data not shown). This is consistent with the fact that homeotropic columnar arrangement is preserved once the two plates are separated. In contrast, after annealing at 183 °C and cooling at room temperature, the initially featureless morphology has completely changed and now shows very large domains containing concentric stripes. As an example, three such domains are partly visible in the 25 × 25 μm^2 height image of Figure 5b. The stripes within the domains are 3−4 nm-high disclinations, yielding a "circuit-like" morphology along with terraces. High-resolution images (for instance, Figure 5c) show the columnar arrangement within the terraces. Individual columns are observed lying perfectly flat on the surface, which means that the columnar arrangement has become planar. The columns are found to be aligned along the axis of the stripes (for instance, along the white double arrow). The two-dimensional (2D) Fourier transform of this image reveals that the columns are 3.9 nm wide, which is in very good agreement with the expected diameter of phthalocyanine molecules. Those columns are thus made of **Pc** molecules that are organized edge-on with respect to the surface plane and packed over long distances. This morphology is similar to that reported in ref 41 for much thinner films (100 nm) obtained by spin-coating. Since our deposits exhibit a thickness ranging from 5 to 20 μm, this indicates that the surface organization of the columns we observe here is not driven by the presence of the substrate but rather by the presence of the open surface.

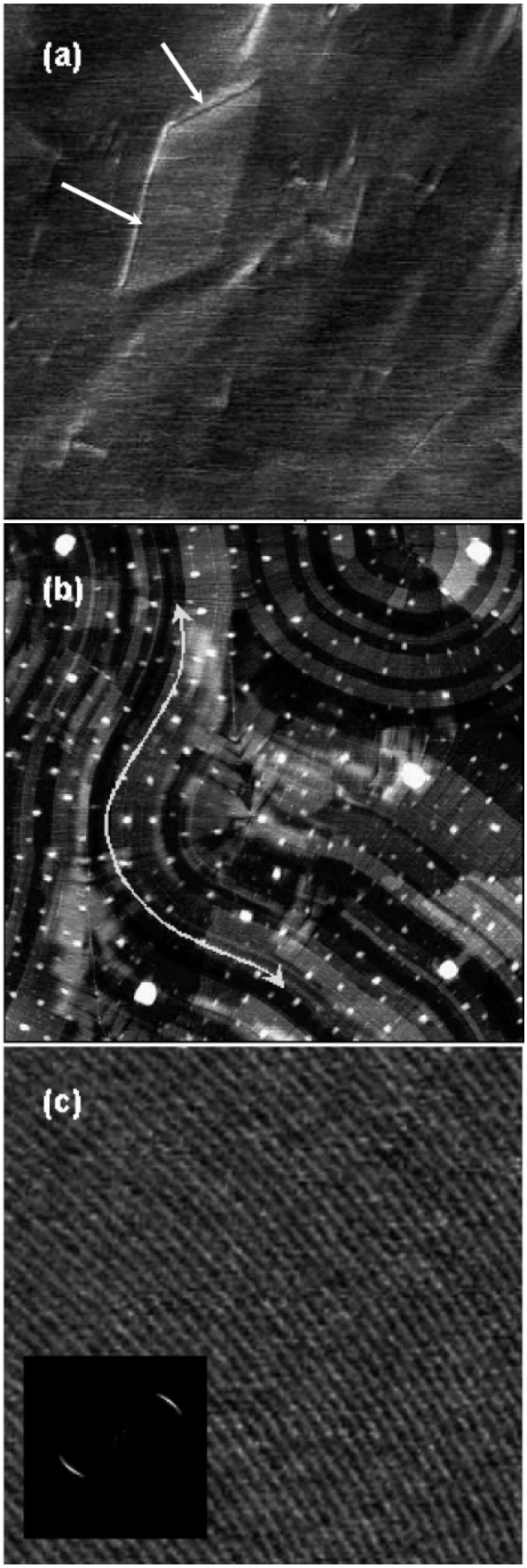

Figure 5. (a) TMAFM phase image (2.5 × 2.5 μm^2) directly after substrate separation. (b) TMAFM height (25 × 25 μm^2) and (c) phase (150 × 150 nm^2) images after annealing.

(41) Gearba, R. I.; Bondar, A. I.; Goderis, B.; Bras, W.; Ivanov, D. A. *Chem. Mater.* **2005**, *17*, 2825−2832.

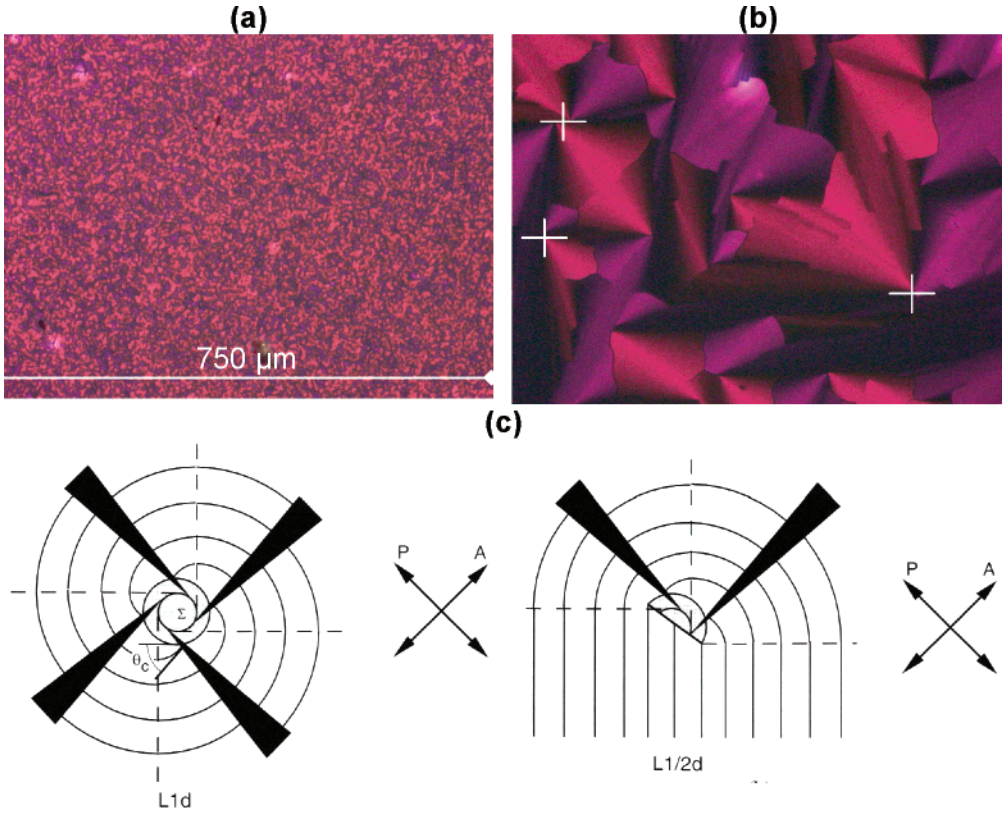

Figure 6. OM images under crossed polarizers of a **Pc** film spin-coated on glass with a thickness of about 200 nm: (a) pristine films, (b) after annealing with a cooling rate of 0.1 °C/min. The white cross indicates the center from which the columns develop, as illustrated schematically in panel c (adapted from reference 28).

The surface of those annealed samples also shows numerous bright dots, rather homogeneous in size, which seem to be regularly distributed over the image (Figure 5b). This is not the usual morphological signature of impurities or contamination, and it is worth noting that no impurities have been detected on these surfaces by XPS. Since those dots are present only after annealing, one explanation might be that they originate from material that could not be accommodated in the columnar stacks during the transition from homeotropic to planar arrangements.

These results show that the effect of thermal annealing on the columnar organization is drastically different if one of the two glass interfaces is removed. While a thermal treatment of the film maintained between two substrates induces homeotropic alignment, it strongly modifies the orientation of the columns from homeotropic to planar when the top substrate is removed. This shows that the natural equilibrium state of the columns is completely different depending on the number of interfaces. To confirm this result, OM and TMAFM measurements have been performed on films prepared on one plate.

3.4. Films Formed on One Plate. OM images recorded under crossed polarizers for 200-nm-thick **Pc** films obtained by spin-coating on a glass plate are presented in Figure 6. Pristine films (Figure 6a) are constituted of small birefringent domains displaying two different colors. Annealing of the films with a cooling rate of 0.1 °C/min leads to the formation of large fan-shaped domains presenting the same colors as the pristine films, separated by extinction branches. When the annealed sample is rotated between the crossed polarizers, the extinction branches rotate as well. Comparable OM textures are observed for pristine and annealed **Pc** films spin-coated on glass substrates, with thicknesses ranging from 50 to 300 nm, and for 200 nm-thick **Pc** pristine and annealed films spin-coated on ITO, PEDOT:PSS, Au, and PCBM substrates (results not shown). Below 50 nm, the films are too thin to display significant birefringence. No influence of the solvent used for spin-coating has been noticed. Pristine **Pc** films spin-coated on FKM present the same morphology as the other pristine films, but they do not resist annealing: as soon as the isotropic phase is reached, the liquid crystal film dewets extensively. This illustrates the high interface tension between the fluorinated polymer and the alkyl chains of the phthalocyanine derivative. This corroborates the hexadecane contact angles, which are similar and small for all the substrates except for FKM, which presents values as high as $\Theta_h = 31°$.

The observation of a highly birefringent texture on glass, ITO, PCBM, gold, and PEDOT:PSS substrates clearly demonstrates that, in contrast to deposits obtained between two substrates, films spin-coated on one substrate do not exhibit homeotropic alignment in the Col_h phase or pseudohomeotropic alignment in the Col_r phase. This is observed both before and after annealing and independently of the nature of the substrate and the thickness of the liquid crystal layer. The fan-shaped texture with extinction branches is characteristic of edge-on orientation of the molecules with curved columns centered on the points, indicated by the white crosses in Figure 6b.[35] This organization is sketched in Figure 6c.

The planar columnar alignment is confirmed by the TMAFM images of a thin film spin-coated on a single glass substrate. Figure 7a,b shows the morphology of a thin film obtained by spin-coating a **Pc** solution (30 mg/mL in toluene) before annealing. In this case, the topography of the deposit consists of numerous elongated structures, for instance, those pointed by the white arrows in Figure 7b. Most of the elongated objects are oriented either parallel or slightly tilted with respect to the substrate surface; they are never perpendicular. Assuming that these "tubes" are bunches of individual **Pc** columns with little long-range ordering, the observed morphology thus suggests that these columns are

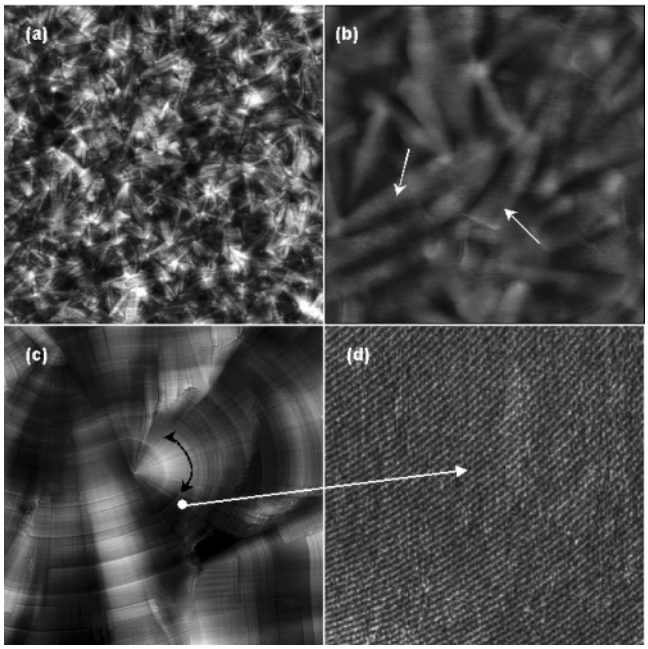

Figure 7. (Top) TMAFM height images 7.5 × 7.5 μm^2 (a) and 1.5 × 1.5 μm^2 (b) of a thin film of **Pc** spin-coated on a glass substrate from a 30 mg/mL toluene solution before annealing. (Bottom) TMAFM height (50 × 50 μm^2) (c) and phase (200 × 200 nm^2) (d) images of the same thin film after annealing.

by far preferentially oriented parallel to the surface rather than perpendicular, meaning that the constitutive disks are preferentially organized edge-on with respect to the surface. These bunches would then correspond to a disorganized edge-on alignment, which is consistent with the OM data showing very small birefringent domains (Figure 6a).

Clearly this situation, in which the columns are poorly organized on the surface, does not reflect an equilibrium situation. Upon annealing, the initially disorganized bunches transform into the same circuit-like morphology observed for the thick films shown before (Figure 7c). Higher resolution images (Figure 7d) confirm that the columns are lying flat on the surface in a concentric manner around growth centers. In this case, the concentration of the spin-coated solution is large enough (30 mg/mL) to generate ∼300 nm-thick films. In contrast, much thinner films of **Pc**, which are typically obtained by spin-coating a 1 mg/mL solution in toluene, exhibit an initial flat morphology made of terraces in which individual PC columns can also be visualized (as also reported in ref 41). However, upon annealing, no further reorganization of the film structure, except dewetting, could be observed.

All these results show that control over the columnar alignment can be exerted by preparing the films either between two substrates or onto a single substrate. This can be explained in the light of the work of Smela et al.[38] The authors demonstrated that the orientation of calamitic molecules deposited on one substrate is influenced to a large extent by the surface tension forces of the air−liquid crystal interface. When the film thickness is smaller than 30 μm, the orientation is entirely dependent on those forces, and calamitic molecules are oriented perpendicular to the air interface, that is, with their alkyl chains pointing to the air interface. A similar explanation can be proposed for our system: interfacial forces occurring at the liquid crystal−air interface strongly favor the planar alignment of columns because the surface tends to be composed exclusively of alkyl side chains, without the presence of the more polar aromatic cores. Those forces overcome the orientational effect of the face-on surface anchoring of the disklike molecules at the film−substrate interface, leading to a texture corresponding to planar alignment. In the two-plate system, where only face-on anchoring of the disklike molecules to the substrates is acting, homeotropic alignment is favored.

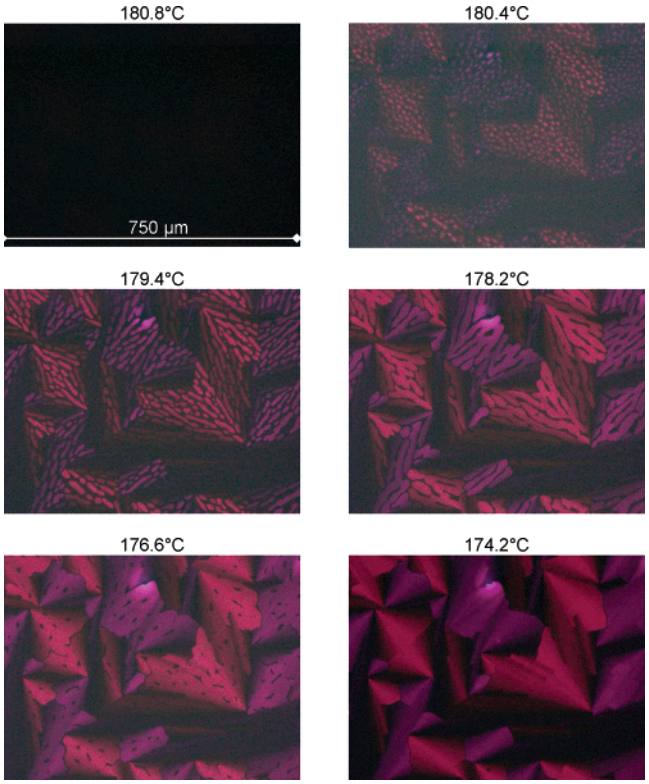

Figure 8. OM images under crossed polarizers of the *I* to Col$_h$ transition occurring in a spin-coated **Pc** film with a thickness of about 200 nm, cooled at a rate of 0.1 °C/min.

The transition from the isotropic phase to the columnar hexagonal (Col$_h$) phase was followed by polarized light microscopy for a 200-nm-thick film spin-coated on glass and annealed at a cooling rate of 0.1 °C/min (Figure 8). The growth of the fan-shaped domains was quite particular since their global shape was already defined at the very early stages by a set of small dots of liquid crystal in the Col$_h$ phase. The growth process then consists mainly in a progressive filling of those domains with the newly formed mesophase. This clearly indicates that the transition starts from the surface of the film. Indeed, from the two-plate experiment, we have seen that the glass surfaces provide homeotropic anchorage to the phthalocyanine. The strong birefringence observed during the transition in thin spin-coated films indicates, on the contrary, that edge-on anchoring is dominant and must be related to the presence of the air−liquid crystal interface. The progressive filling of the domains can be interpreted as the continuous thickening of the organized layers, starting from the air−liquid crystal interface and directed toward the liquid crystal−glass interface. This phenomenon was also observed with X-ray diffraction for nematic liquid crystals.[42] The authors showed that, in films with a thickness higher than 12 molecular layers, two transitions from *I* to *N* were observed: one at higher temperature for the surface, and another one at lower temperature for the bulk of the material. This can be understood easily by the fact that molecules at the air−liquid crystal interface sustain a large driving force for edge-on ordering (alkyl chains tend to orient toward air to reduce the free energy of the surface). As a consequence, the first layers of the liquid

(42) Moncton, D. E.; Pidak, R.; Davey, S. C.; Brown, G. S. *Phys. Rev. Lett.* **1982**, *49* (25), 1865−1868.

crystal in the isotropic phase are more ordered than the bulk and are able to order at higher temperature. This phenomenon, called surface freezing, is well documented for *n*-alkanes.[43] Since **Pc** is composed of more than 80% alkyl chains, it is not surprising that its surface behavior is governed by its alkyl moieties.

4. Conclusions

We demonstrated that, for the **Pc** molecule used in this study, the control of columnar alignment is determined by the confinement induced by solid substrates rather than by the nature of those substrates. Indeed, if a **Pc** film is spin-coated on a substrate, whatever its surface energy or roughness, a planar alignment is always observed. This can be explained by the fact that forces acting at the liquid crystal−air interface favor planar alignment, and they overcome the face-on anchoring of disk mesogens acting at the DLC−substrate interface. It was also demonstrated that the planar alignment observed for films deposited on one substrate develop, upon cooling from the isotropic phase, from the air interface. This is due to a phenomenon called surface freezing, which induces the preferential orientation, already in the isotropic phase, of the alkyl chains of **Pc** toward air. On the contrary, if the **Pc** film is confined between two identical substrates, whatever their surface energy or roughness, homeotropic alignment is observed in most cases. The columnar organization, that is, planar versus homeotropic, deduced from the OM images was confirmed at the nanometer scale by TMAFM observations. Single curved columns, forming concentric circles, were resolved in the case of planar alignment.

Acknowledgment. This work was supported by the Communauté Française de Belgique (ARC 00/05-257), the Walloon Region PIMENT program (SOLPLAST project), the Belgian Federal Science Policy Office (SOLTEX PAT project and PAI 5/3), the European Commission (NAIMO NMP4-CT-2004-500355 and Phasing-Out Hainaut), and the Belgian National Fund for Scientific Research (FNRS). We are much indebted to Michel Hecq, Jean-Pierre Dauchot, and Axel Hemberg for the preparation of the gold substrates, and to Phil Mackie for inductively coupled plasma optical emission spectroscopy (ICP-OES) measurements.

Supporting Information Available: ICP-OES and XPS analyses. This material is available free of charge via the Internet at http://pubs.acs.org.

LA0605182

(43) Sloutskin, E.; Bain, C. D.; Ocko, B.; Deutsch, M. *Faraday Discuss.* **2005**, *129*, 339−352.